The Latency Information Theory Revolution, Part III: Knowledge-Unaided Power-Centroid Adaptive Radar

Erlan H. Feria
Department of Engineering Science and Physics
The College of Staten Island of the City University of New York
E-mail feria@mail.csi.cuny.edu Web site http://feria.csi.cuny.edu

Abstract—Knowledge unaided power centroid (KUPC) adaptive radar and its latency information theory (LIT) roots are reviewed in this third paper of a three paper series. LIT is the universal guidance theory for efficient system designs that has inherently surfaced from the confluence of five ideas. They are: 1) The source entropy and channel capacity performance bounds of Shannon's mathematical theory of communication; 2) The latency time (LT) certainty of Einstein's relativity theory; 3) The information space (IS) uncertainty of Heisenberg's quantum physics; 4) The black hole Hawking radiation and its Boltzmann thermodynamics entropy $\boldsymbol{S}$ in SI J/K; and 5) The author's 1978 conjecture of a structural-physical LT-certainty/IS-uncertainty duality for stochastic control. LIT is characterized by a four quadrants revolution. While the first and third quadrants are concerned with the life time of physical signal movers and the life space of physical signal retainers, respectively, the second and fourth quadrants are about the intelligence space of mathematical signal sources and the processing time of mathematical signal processors, respectively. The four quadrants of LIT are assumed to be physically independent with their system design methodologies guided by dualities and performance bounds. Moreover, all the LIT quadrants are bridged by statistical physics, inclusive of a recently discovered time dual for thermodynamics that has been named lingerdynamics. The theoretical and practical relevance of LIT has already been demonstrated using real-world control, physics, biochemistry and the KUPC adaptive radar application that is reviewed in this paper. KUPC adaptive radar is a technique that falls within the fourth quadrant of LIT, and is thus a mathematical signal processing technique whose goal is the efficient detection of moving targets in real-world taxing environments. As is highlighted in this review KUPC adaptive radar is found to come relatively close to the signal to interference plus noise ratio (SINR) radar performance of DARPA's knowledge-aided sensory signal processing expert reasoning (KASSPER) even though it is knowledge unaided.

Index Terms—Latency-certainty, information-uncertainty, mathematical-intelligence, physical-life, adaptive radar, knowledge unaided, DARPA, KASSPER, signal processor, structural-physical latency-certainty/information-uncertainty duality

1. Introduction

This paper succinctly reviews the origins of the powerful and fast knowledge-unaided power-centroid (KUPC) adaptive radar scheme [1]. This scheme systematically arose as an application of the nascent latency information theory (LIT) system design guidance philosophy of [2]-[4] to the derivation of a simple alternative to the 2001-2005 DARPA's knowledge-aided sensory signal processing expert reasoning (KASSPER) program [5]. In Section 2 the chronological development of LIT is documented up to the development of KUPC adaptive radar. In Section 3 the airborne moving target indicator (AMTI) adaptive radar problem is stated whose solution the KUPC adaptive radar algorithm efficiently addresses without the need for prior knowledge. In the last section the signal to interference plus noise ratio (SINR) radar performance of three alternative adaptive radar techniques are contrasted with that of KUPC adaptive radar.

2. The Latency Information Theory Roots of KUPC Adaptive Radar

LIT consists of a four quadrants revolution whose chronological development is documented next. The discussion starts with the statement of the two lossless efficiency performance bounds of the mathematical theory of communication [6] which is part of information theory. Since the units of communicated source information are mathematical bits, classical information theory is referred in LIT as mathematical information theory (or MIT), where

This work was supported in part by the Defense Advanced Research Projects Agency (DARPA) under Grant No. FA8750-04-1-004 and the PSC-CUNY Research Awards PSCREG-37-913, 38-247, 39-834, 40-1013, 41-951

Mobile Multimedia/Image Processing, Security, and Applications 2010, edited by Sos S. Agaian, Sabah A. Jassim,
Proc. of SPIE Vol. 7708, 77080V · © 2010 SPIE · CCC code: 0277-786X/10/$18 · doi: 10.1117/12.849716

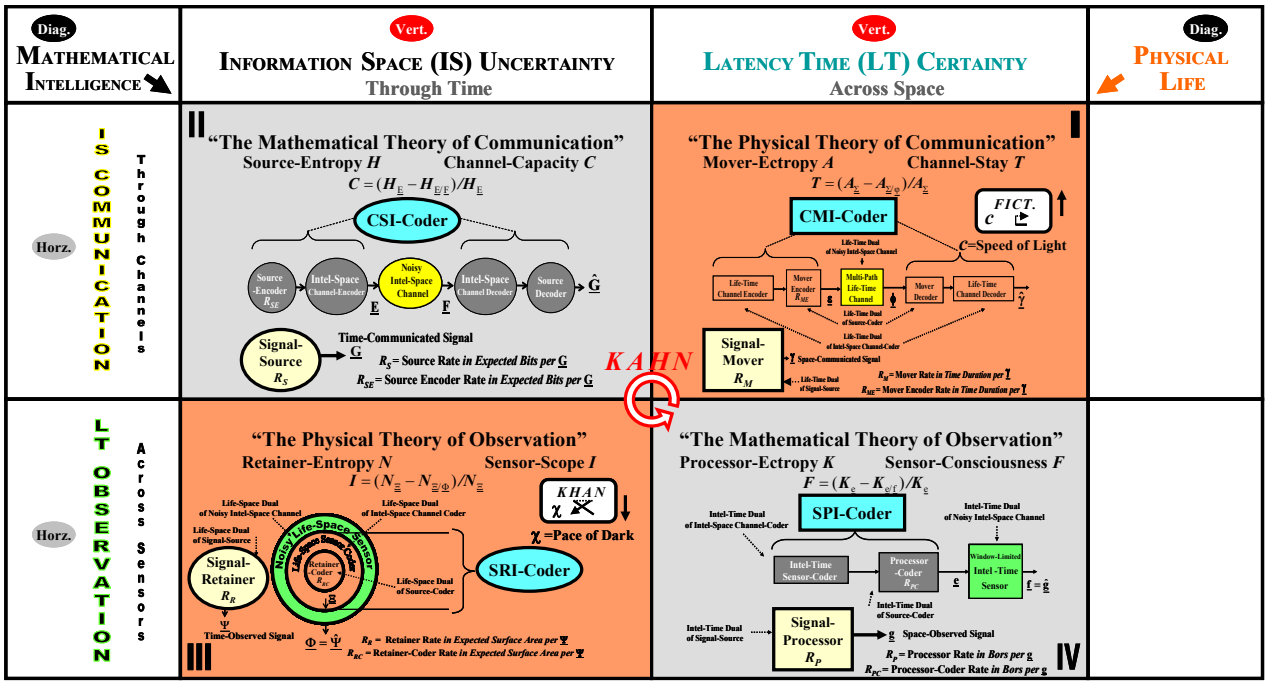

Fig. 1. The Structural-Physical LT-Certainty/IS-Uncertainty Dualities of the LIT Revolution.

MIT is in quadrant II. In this way MIT can be contrasted with the nascent physical information theory (PIT) of quadrant III where the units of the observed physical retainer information are SI square meters. The same kind of contrast can be made between 'the mathematical theory of communication' of Shannon and 'the physical theory of observation' of quadrant III that guides the efficient use of life space in SI m^2 units by physical signal retainers via two lossless performance bounds. However in this paper PIT is not used since it is unrelated to the KUPC adaptive radar algorithm. Moreover, for similar reasons, the physical latency theory (PLT) which is in quadrant I of LIT and uses 'the physical theory of communications' to guide the efficient use of life time in SI secs units by physical signal movers [2]-[4] is not treated here. Next in chronological order the assumed structural-physical latency time (LT) certainty/information space (IS) uncertainty duality of 1978 by the author for stochastic control will be reviewed. This assumption was the catalyst to the search and discovery of a time dual for MIT that had similar structural-physical properties. This time dual was called mathematical latency theory (MLT), appearing in quadrant IV of LIT, which was concerned with the efficient use of processing time in binary operator (bor) units by signal processors via 'the mathematical theory of observation' also using two lossless performance bounds. Next the 2004-2005 University Grant from DARPA's KASSPER program [7] is discussed that motivated the discovery of MLT and as mentioned earlier led to the development of KUPC adaptive radar. Finally, the performance bounds and structural-properties of MLT are briefly discussed for ease of reference.

A. The Two Performance Bounds of The Mathematical Theory of Communication of LIT's MIT

The first lower performance bound of MIT is used to guide the design of source-coders and is denoted as the source-entropy with symbol $\boldsymbol{H}$ in bit units [6] for the sourced intelligence space (or intel-space in short) quantity that it represents. More specifically $\boldsymbol{H}$ is defined as the expected source-information

$$\boldsymbol{H} = E[I_S(\underline{g}_i)] = \sum_{i=1}^{\Omega} P_S(\underline{g}_i) I_S(\underline{g}_i) \text{ in bit units} \quad (1)$$

$$I_S(\underline{g}_i) = \log_2(1/P_S(\underline{g}_i)) \quad (2)$$

where: 1) $\underline{G} \in \{\underline{g}_1,..\underline{g}_\Omega\}$ is a n-dimensional random vector composed of Ω vector outcomes $\{\underline{g}_1,..\underline{g}_\Omega\}$; 2) $I_S(\underline{g}_i)$ is the $\underline{g}_i$ source-information in bit units; 3) $P_S(\underline{g}_i)$ is the $\underline{g}_i$ source-probability; and 4) $\boldsymbol{H}=\log_2\Omega$ is the maximum possible source-entropy that occurs when the outcomes are equally likely.

The second and upper MIT performance-bound is used to guide the design of the channel and source integrated (CSI) coder shown in quadrant II of the LIT revolution of Fig. 1. While the source-coder of the CSI-coder efficiently compresses intel-space, its channel-coder efficiently uses overhead intel-space for the time-communication of intel-

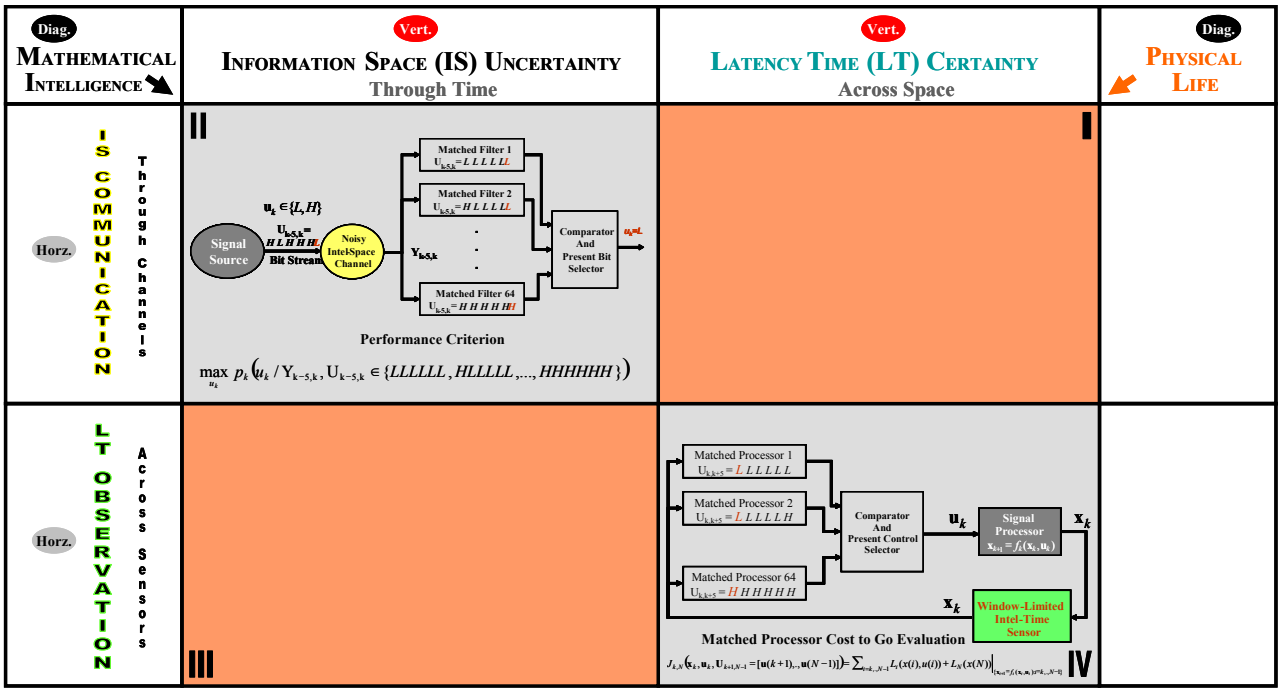

Fig. 2. The LIT revolution display of IS-uncertainty detection and LT-certainty quantized control.

space through a noisy intel-space channel. The CSI-coder's performance bound is called channel-capacity with symbol $\boldsymbol{C}$ and denotes the maximum percentage of intel-space extracted without loss from a noisy intel-space channel. $\boldsymbol{C}$ is thus defined as

$$0 \le \boldsymbol{C} = (\boldsymbol{H}_{\underline{E}} - \boldsymbol{H}_{\underline{E}/\underline{F}})/\boldsymbol{H}_{\underline{E}} = \max_{\{P_S[e_i]\}} [(\boldsymbol{H}_{\underline{E}} - \boldsymbol{H}_{\underline{E}/\underline{F}})/\boldsymbol{H}_{\underline{E}}] \le 1 \tag{3}$$

where $\underline{E}$ is the input and $\underline{F}$ is the output of the channel corresponding to the n-dimensional codewords $\underline{e}$ and $\underline{f}$ with a source-probability distribution $\{P_S[e_i]\}$ that maximizes the mutual source-information $(\boldsymbol{H}_{\underline{E}} - \boldsymbol{H}_{\underline{E}/\underline{F}})/\boldsymbol{H}_{\underline{E}}$ (e.g., for a memoryless symmetric channel $\{P_S[e_i]\}$ is uniformly distributed, i.e., $P_S[e_1]=P_S[e_2]=1/2$). In particular, $\boldsymbol{H}_{\underline{E}/\underline{F}}$ can be viewed as a *channel-induced intel-space penalty* whose value determines the percentage of the intel-space specified by $\boldsymbol{H}_{\underline{E}}$ that can be time-communicated without loss (or equivalently its probability of error approaches zero).

B. The Structural-Physical LT-Certainty/IS-Uncertainty Duality Conjecture

The structural-physical LT-certainty/IS-uncertainty duality conjecture of 1978 gave rise to the mathematically tractable separation of stochastic quantized control designs into a LT-certainty processor-state control evaluator design and an IS-uncertainty processor-state estimator design [8]. In particular, this approach resulted in a Matched Processors methodology for quantized control [9] which was derived as the LT-certainty dual of the IS-uncertainty Matched Filters methodology [10] for the detection of transmitted bits through a noisy intel-space channel. More specifically, given observations of the present state of the controlled signal-processor (modeled with deterministic state equations), matched processors evaluated for a small set of present and future quantized controls the cost to go for each control sequence. From these matched processor evaluations the present control was then found that yielded the best cost to go for a suitable horizon, and its value applied to the controlled signal-processor. The approach was repeated as many times as there were control steps. It is of interest to note that besides Matched Processors being rather straight forward, it also has the fundamental advantage of not suffering from 'the curse of dimensionality' of the alternative control methodology, i.e., Bellman's Dynamic-Programming [11] since the number of required matched processors for practical applications can be very small [8]. In Fig. 2 the Matched Processors control structure for the control of a signal processor (or plant) is shown on the LT-certainty/LT-observation quadrant IV of the LIT revolution, while its structural dual, i.e. the Matched Filters detector structure for the detection of bits [10], is shown on the IS-uncertainty/IS-communication quadrant II.

C. The DARPA University Grant

The merging of MIT with the structural-physical LT-certainty/IS-uncertainty duality of Fig. 2 to yield mathematical latency theory (or MLT) was motivated by a university grant from DARPA [7]. The objective of this research was to use minimum mean square error predictive-transform (MMSE-PT) source coding [12] for the lossy compression of synthetic aperture radar (SAR) imagery of the earth, later to be used in a knowledge-aided adaptive radar [13] system subjected to severely taxing environmental disturbances. This problem turned out to be extremely difficult to address since in addition to the compression of the SAR imagery, the *processing time* of the associated adaptive airborne moving target indicator (AMTI) radar 'lossless' signal-processor also needed to be radically compressed. Moreover, it was also found that regardless of how fast a lossless signal-processor was, it could never be suitably matched to its input when it consisted of compressed SAR imagery that was both radar-blind and highly-lossy. This lack of match between the lossless signal-processor and its compressed input, results in an unsatisfactory signal to interference plus noise ratio (SINR) radar performance. Fortunately, however, this problem was then solved by once again invoking the Matched Processors structural-physical LT-certainty/IS-uncertainty duality conjecture of Fig. 2. In this latest revelation while the compression of intel-space is an IS-uncertainty/IS-communication problem, the compression of intel-time is a LT-certainty/LT-observation one. Moreover and just as importantly, since the LT-certainty Matched Processors methodology was structurally similar to that of the IS-uncertainty Matched Filters methodology, it was felt that the IS-uncertainty/IS-communication MIT system design methodology of quadrant II must also have a 'LT-certainty signal-processor design methodology' with dual strategies. In this way MLT inherently surfaced as the LT-certainty/LT-observation dual of IS-uncertainty/IS-communication MIT. Of all the inherited MLT strategies the most compelling one was the appearance of 'lossy' processor-coders. After this property was identified it was then applied to the design of a suitably lossy adaptive AMTI radar signal-processor. More specifically, the clutter covariance evaluator whose input was the stored SAR imagery was replaced with a lossy power-centroid clutter processor. This highly lossy clutter covariance evaluator first determined from the stored SAR imagery the power and power-centroid values of the investigated clutter range-bin. Using these values, it then extracted a suitable clutter covariance from a small set, earlier designed off-line and stored in memory. After this approach was tried it was found that besides being extremely fast, the processor resulted in outstanding SINR radar performances while using stored SAR imagery that was both radar-blind and exceedingly lossy. The lossy SAR imagery resulted from the compression of the lossless SAR imagery by a factor of 8,172. Moreover, an even more surprising result later surfaced [1]. It was that a lossy adaptive AMTI radar signal-processor algorithm can be designed that emulates the outstanding SINR radar performance of the former scheme without the need of clutter prior-knowledge, i.e., SAR imagery. This highly desirable result surfaced from the discovery that both the range-bin power and its power-centroid can be readily derived from the on-line sample covariance matrix.

D. The Two Performance Bounds of The Mathematical Theory of Observation of LIT's MLT

Similarly to the mathematical theory of communication of MIT, the mathematical theory of observation of MLT has two performance bounds that guide system designs. The first is the lower performance bound for processor-coder designs, which is called processor-ectropy with symbol $\boldsymbol{K}$ and values given in binary operator (bor) units for the processing intelligence time (or intel-time for short) levels that it represents. A processor-coder is any replacement of the original signal-processor whose output is said to be lossless when it matches that of the original signal-processor and lossy when it does not. More specifically $\boldsymbol{K}$ is a minimax criterion that is illustrated next with a simple example. This example is of a 1-bit full-adder [14] original signal-processor that has a slow bor multi-level implementation structure where the sum output is associated with six bor levels and the carry-out with five bor levels. The reason for this relatively large number of bor levels is that this full-adder only uses two-input gates. However, for this example it is found that $\boldsymbol{K}$ =3 bors since the minimum number of bor levels needed to generate the carry bit is two, and for the sum bit is three as is noted to be the case when a 'sum of minterms' implementation methodology is used [14] and more than two-input gates are allowed. While the 1-bit full adder is a lossless processor-coder, a lossy but faster, by one bor level, 1-bit full adder can be readily derived from the lossless case by only implementing the two bor levels for the carry out and by setting the sum output to zero. $\boldsymbol{K}$ is thus defined as

$$\boldsymbol{K} = \max[L_P(g_1),..,L_P(g_N)] = \max[f_1[C_P(g_1)],..,f_N[C_P(g_N)]] \tag{4}$$

where: a) $\underline{g}=[g_1,..g_N]$ is the N-dimensional signal-processor vector output; b) $L_P(g_i)$ is the g_i processor-latency, e.g. $L_P(sum)=3$ bors for the full-adder; and c) $f_i[C_P(g_i)]=L_P(g_i)$ conveys $L_P(g_i)$ dependence on the g_i processor-constraint $C_P(g_i)$.

The second and upper MLT performance bound is used to guide the design of the sensor and processor integrated (SPI) coder shown in quadrant IV of the LIT revolution of Fig. 1. While the SPI-coder's processor-coder efficiently compresses intel-time, its sensor-coder efficiently uses overhead intel-time for the space-observation of intel-time across a window-limited intel-time sensor. The SPI-coder's performance bound is called sensor-consciousness with symbol $\boldsymbol{F}$ and denotes the maximum percentage of the mathematical latency extracted without loss from a window-limited intel-time sensor. Thus $\boldsymbol{F}$ is defined by

$$0 \le \boldsymbol{F} = (\boldsymbol{K}_{\underline{\mathbf{e}}} - \boldsymbol{K}_{\underline{\mathbf{e}}/\underline{\mathbf{f}}})/\boldsymbol{K}_{\underline{\mathbf{e}}} = \max_{\{C_P[e_i]\}} [(\boldsymbol{K}_{\underline{\mathbf{e}}} - \boldsymbol{K}_{\underline{\mathbf{e}}/\underline{f}})/\boldsymbol{K}_{\underline{\mathbf{e}}}] \le 1 \tag{5}$$

where $\underline{\mathbf{e}}$ is the input and $\underline{\mathbf{f}}$ is the output of the sensor corresponding to the n-dimensional vectors $\underline{\mathbf{e}}$ and $\underline{f}$ with processor-constraints $\{C_P[e_i]\}$ that maximize the mutual processor latency $(\boldsymbol{K}_{\underline{\mathbf{e}}} - \boldsymbol{K}_{\underline{\mathbf{e}}/\underline{f}})/\boldsymbol{K}_{\underline{\mathbf{e}}}$ (e.g., for the full adder case the processor constraints $\{C_P[e_i]\}$ that maximize the mutual processor latency is when the sum output and carry-out can be derived using logic gates with an arbitrary number of inputs). In particular, $\boldsymbol{K}_{\underline{\mathbf{e}}/\underline{\mathbf{f}}}$ is a *sensor-induced intel-time penalty* whose value determines the percentage of the intel-time specified by $\boldsymbol{K}_{\underline{\mathbf{e}}}$ that can be space-observed without loss. In Fig. 2d the SPI-coder is displayed whose design is guided by $\boldsymbol{F}$. As an illustration of how (5) can be used in SPI-coder designs consider a 1-bit full-adder based recursive adder of two bytes. This recursive adder has a processor-ectropy of 16 bors, i.e., $\boldsymbol{K}_{\underline{\mathbf{e}}}$=16 bors, since the processor-latency of the 1-bit full-adder carry-out is of 2 bors and 8 bit pairs (plus the associated carry-in) are being added. Then if one observes the adder output with a 14-bors window-limited intel-time sensor, the sensor-induced inter-time penalty will be of 2 bor, i.e. $\boldsymbol{K}_{\underline{\mathbf{e}}/\underline{\mathbf{f}}}$ =2 bors. In turn, this results in a sensor-consciousness value of $\boldsymbol{F}$=(16-2)/16=0.88 that informs us that only 88% of the 16 bors intel-time of $\boldsymbol{K}_{\underline{\mathbf{e}}}$ can be space-observed without loss. Thus the adder intel-time latency must be of at least 18 bors. The additional 2 bors that are required to observe the full sum can then be facilitated by a sensor-coder that uses prior-knowledge, e.g. that LSBs can be zero, which allows the addition to start 2 bors earlier in time.

3. The Airborne Moving Target Indicator (AMTI) Adaptive Radar System

In this section the airborne moving target indicator (AMTI) adaptive radar problem is discussed and its mathematical modeling is reviewed. The discussion starts with Fig. 3 where an airborne Boeing 767 is shown together with a typical 4 Megabytes SAR image of the Mojave Airport in California. The 767 is assumed to carry an AMTI adaptive radar system whose task is to investigate the location at the clutter range-bin boresight angle θ_C of 0^o that is miles away to determine if a moving target appears there. On the other hand, the SAR image represents clutter prior knowledge that is made available to the radar system to facilitate its detection of targets.

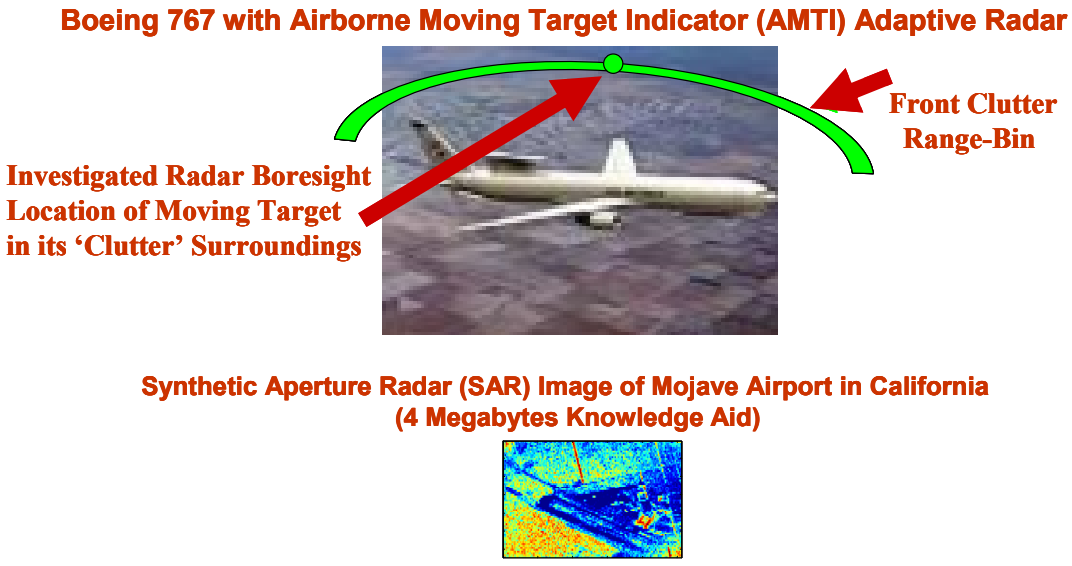

Fig. 3. Airborne Moving Target Indicator (AMTI) Adaptive Radar With SAR Image Knowledge Aid.

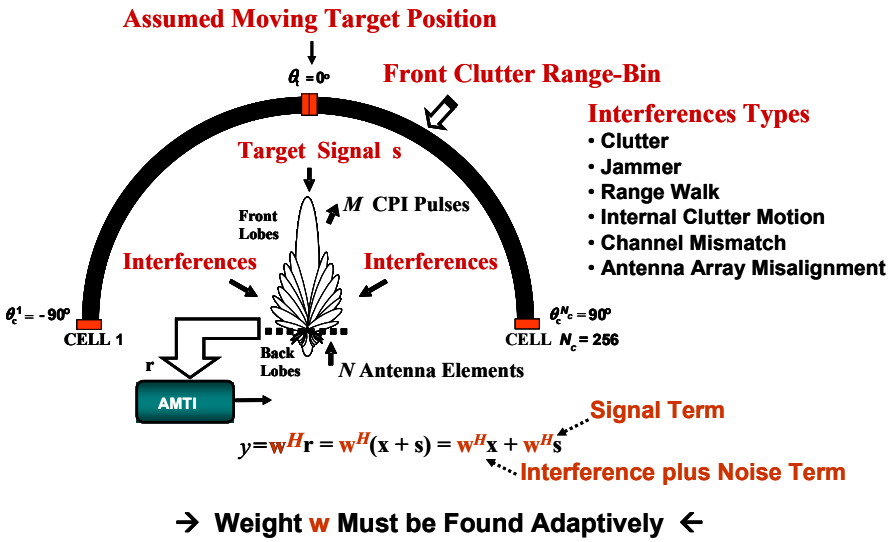

Fig. 4. An Overview of the Radar System Mathematical Model.

Next in Fig. 4 a mathematical idealization of the AMTI adaptive radar problem is presented where all the technical details are found in [1]:

- The AMTI system receives as an input the pulse returns from the range bin via an array of N antenna elements that also send M pulses towards the range bin during a coherent pulse interval (CPI). The antenna pattern associated with the pulse transmissions is also shown in the figure where the front mainlobe/sidelobes are significantly more powerful than the back ones. In the simulation results to be discussed later it was assumed that: 1) the value of N is 16; 2) the value of M is 16; 3) the constant front antenna gain is of 56 dBs; and 4) the constant back antenna gain is of -40 dBs [1].
- The front range bin is assumed to consist of N_C =256 clutter cells.
- The target signal return is assumed normalized and given by its steering vector **s** which is a complex 256-dimensional vector.
- The signal return **x** is a complex 256-dimensional vector that results from the addition of all the signal interferences and antenna thermal noise.
- The assumed types of interferences appearing in the AMTI input **x** are: 1) clutter; 2) jammer; 3) range walk; 4) internal clutter motion; 5) channel mismatch; and 6) antenna array misalignment.
- The total input to the AMTI is given by the addition of **x** and **s**.
- The AMTI performs the inner product multiplication of a complex 256-dimensional weighting vector **w** and its total input to yield the complex scalar output $y=\mathbf{w}^H(\mathbf{x}+\mathbf{s})= \mathbf{w}^H\mathbf{x}+\mathbf{w}^H\mathbf{s}$ where: 1) the exponent 'H' denotes a complex transpose and conjugation; 2) the term $\mathbf{w}^H\mathbf{x}$ is the interference plus noise component of y; and 3) the term $\mathbf{w}^H\mathbf{s}$ is denoted as the signal component of y.
- A high performance adaptive algorithm must be found that modifies the weighting vector **w** as the interference characteristics change. To address this problem the signal to interference plus noise ratio ($SINR$) performance criterion

$$SINR = \mathbf{w}^H \mathrm{ss}^H \mathbf{w} / \mathbf{w}^H R_{xx} \mathbf{w} \tag{6}$$

is maximized with respect to **w** where R_{xx} is the interference plus noise covariance

$$R_{xx} = E[\mathbf{x}^H \mathbf{x}]. \tag{7}$$

The result of this maximization yields

$$SINR_{Opt} = \max_{\mathbf{w}}\left(\mathbf{w}^H \mathrm{ss}^H \mathbf{w} / \mathbf{w}^H R_{xx} \mathbf{w}\right) = \mathbf{w}_{Opt}^H R_{xx}^{-1} \mathbf{w}_{Opt} = \mathbf{s}^H R_{xx}^{-1} \mathbf{s} \tag{8}$$

where the optimum weighing vector $\mathbf{w}_{\mathrm{Opt}}$ is given by the Wiener-Hopf equation

$$\mathbf{w}_{Opt} = R_{xx}^{-1}\mathbf{s}\,. \tag{9}$$

This result in turn tell us that to achieve the best possible SINR adaptive radar performance our efforts should be concentrated in the on-line derivation of the interference plus noise covariance R_{xx}. In the next section four algorithms that determine R_{xx} adaptively, inclusive of KUPC adaptive radar, are reviewed.

4. A Comparative Study

Next four adaptive radar schemes are compared. The first is the knowledge-unaided sample covariance matrix inverse (SCMI) algorithm [1] that is characterized by its simplicity but yields a poor SINR radar performance. The second is the 2001-2005 knowledge-aided KASSPER algorithm that is characterized by an excellent SINR radar performance but is unfortunately rather complex. The third is the 2006 knowledge-aided power-centroid (KAPC) algorithm that while being much simpler emulates the KASSPER algorithm SINR radar performance. The last is the 2009 KUPC algorithm that while emulating the SINR radar performance of the KASSPER and KAPC algorithms is much simpler to implement since prior knowledge in the form of SAR imagery is unnecessary.

A. The Sample Covariance Matrix Inverse (SCMI) Algorithm

The SCMI algorithm is conveniently summarized in Fig. 5 where the NMxNM dimensional complex interference plus noise covariance matrix $\hat{R}_{xx}$ is constructed from the addition of the sample average sum $\sum_{i=1}^{K} \mathrm{X}_i \mathrm{X}_i^{\mathrm{H}} / K$ and the diagonal loading factor $\sigma_{Diag}^2 I$ where: 1) the set $\{\mathrm{X}_i: i=1,..,K\}$ consists of K measured complex NM-dimensional column vector samples where NM=256 in our simulations: 2) the loading factor $\sigma_{Diag}^2 I$ is adjusted to a value that avoids numerical stability problems associated with the inversion of $\hat{R}_{xx}$, in our simulations it is assumed that $\sigma_{Diag}^2 I = 10I$; and 3) the samples $\{\mathrm{X}_i: i=1,..,K\}$ only include measurements from range-bins that are adjacent to the range-bin under investigation to avoid possibly significant target interference effects.

$$\hat{R}_{xx} = \frac{1}{K}\sum_{i=1}^{K}\mathbf{X}_i\mathbf{X}_i^H + \sigma_{Diag}^2 I = \begin{bmatrix} X & X & X & X & \cdots & X & X & X & X \\ X & X & X & X & \cdots & X & X & X & X \\ X & X & X & X & \cdots & X & X & X & X \\ X & X & X & X & \cdots & X & X & X & X \\ \vdots & \vdots & \vdots & \vdots & \ddots & \vdots & \vdots & \vdots & \vdots \\ X & X & X & X & \cdots & X & X & X & X \\ X & X & X & X & \cdots & X & X & X & X \\ X & X & X & X & \cdots & X & X & X & X \\ X & X & X & X & \cdots & X & X & X & X \end{bmatrix}$$

Fig. 5. The SCMI Algorithm.

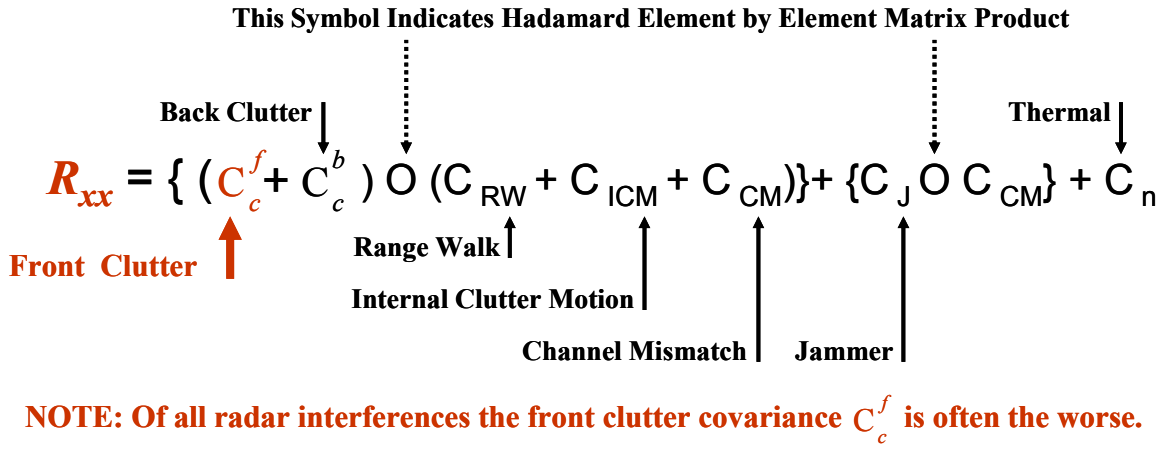

Fig. 6. The KASSPER Interference Plus Noise Correlation Matrix.

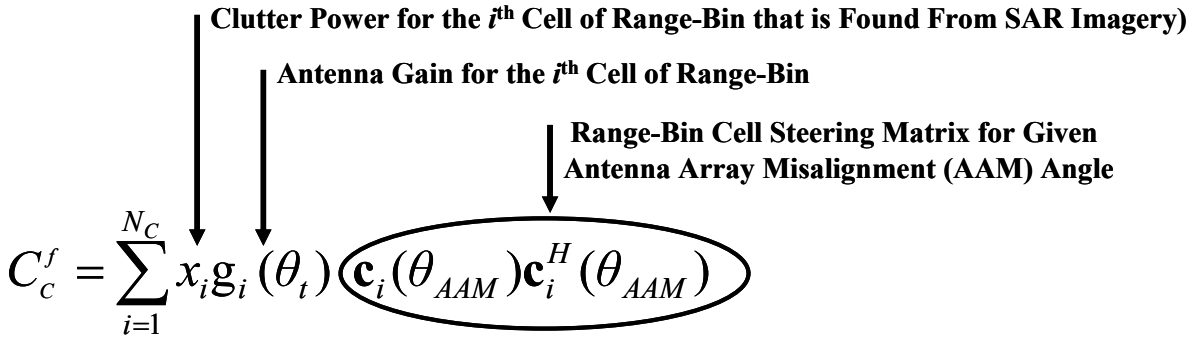

Fig. 7. The KASSPER Front Clutter Covariance.

B. The 2001-2005 KASSPER Algorithm

The KASSPER algorithm investigated [7] is conveniently summarized in Figs. 6 and 7 where the NMxNM dimensional complex interference plus noise covariance matrix R_{xx} is assumed perfectly known and given by the expression shown in Fig. 6 that is discussed in detail in [1]. In particular, all the covariance matrices shown in Fig. 6 are generally complex and of dimension NMxNM where: 1) C_n is the thermal covariance of the radar system; 2) C_J is the jammer covariance; 3) C_{CM} is the channel mismatch covariance; 4) C_{RW} is the range walk covariance; 4) C_{ICM} is the internal clutter motion covariance; 5) C_c^b is the back clutter covariance which is assumed negligible in our simulations since the power of the back mainbeam/sidelobes of the antenna pattern is relatively small; and 6) C_c^f is the front clutter covariance which is evaluated making use of the stored SAR imagery. In Fig. 7 the expression used to evaluate C_c^f is stated where: 1) x_i is the real scalar clutter power of the i^{th} range-bin cell; 2) $\mathbf{c}_i(\theta_{AAM})$ is the complex steering vector of NM-dimension for the i^{th} range-bin cell with θ_{AAM} being the angular amount of antenna array misalignment; and 3) $g_i(\theta_t)$ is the antenna gain associated with the i^{th} range-bin cell, that is linked to an antenna pattern pointing towards the angular location of the investigated target θ_t on the range-bin. It is assumed here that the antenna pattern is given by the analytical expression

$$g_i(\theta_t) = K^f \left| \frac{\sin\left\{ N\pi \frac{d}{\lambda}(\sin(\theta_C^i) - \sin(\theta_t)) \right\}}{\sin\left\{ \pi \frac{d}{\lambda}(\sin(\theta_C^i) - \sin(\theta_t)) \right\}} \right|^2 / N^2 \quad (10)$$

where θ_t is the target boresight angle, d is the antenna inter-element spacing, λ is the operating-wavelength, and K^f is the front antenna gain constant.

C. The 2006 Knowledge-Aided Power-Centroid (KAPC) Algorithm

The KAPC algorithm is conveniently summarized in Figs. 8 thru 12 where the NMxNM dimensional complex interference plus noise covariance matrix ${}^{KAPC}R_{xx}$ shown in Fig. 8 is identical to the KASSPER R_{xx} of Fig. 6 except for the front clutter covariance matrix ${}^{KAPC}C_c^f$. More specifically, the front covariance matrix is given by the product of the real scalar range-bin power RB_P and a compensation antenna pattern (CAP) normalized front clutter covariance ${}^{CAP}C_c^f(Q(RB_{PC}))$ where: 1) RB_P is the power of the range-bin defined in Fig. 9 with the assumption that there are 256 range-bin cells and the antenna pattern of (10) is directed towards the middle 128 range-bin cell; 2) RB_{PC} is the power-centroid of the range-bin defined in Fig. 10 with its value being equal to 128 for stationary clutter; 3) in Fig. 11 RB_P and RB_{PC} have been plotted for the 64 range bins constructed from the SAR image of the Mojave Airport in California. Moreover, these plots are not far from those obtained with the 512 bytes MMSE PT compressed SAR image also shown in Fig. 10; 4) $Q(RB_{PC})$ denotes the quantization of the range-bin power centroid RB_{PC} as illustrated in Fig. 12 for three quantization levels, i.e., 64, 128 and 192; 5) ${}^{CAP}C_c^f(Q(RB_{PC}))$ is defined in Fig. 12 and consists of first creating an antenna pattern from (10) that is directed towards $Q(RB_{PC})$ and then using these results to create a predicted covariance matrix, i.e., ${}^{CAP}C_c^f(Q(RB_{PC}))$; and 6) the off-line determined NMxNM complex covariance matrix ${}^{CAP}C_c^f(Q(RB_{PC}))$ can then be stored for all cases of $Q(RB_{PC})$ in a memory and later retrieved to determine ${}^{KAPC}C_c^f$ as the need arises based on the determined value for $Q(RB_{PC})$. The advantage of this technique over the KASSPER scheme is that the radar-blind and highly compressed SAR image of Fig. 11 can be readily used to yield an excellent estimate of the power and power-centroid of the range-bin which is all that is needed to determine ${}^{KAPC}C_c^f$.

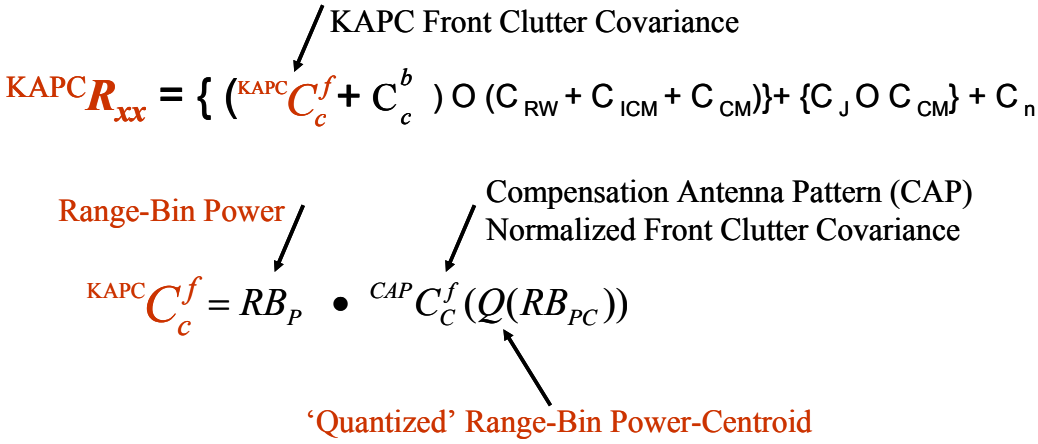

Fig. 8. The KAPC Interference Plus Noise Covariance.

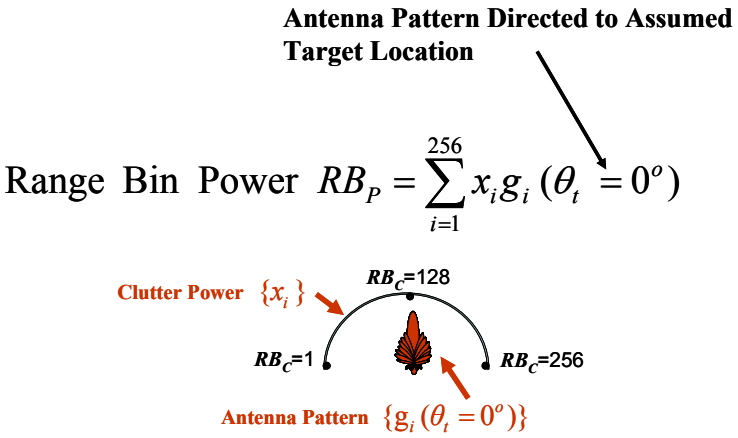

Fig. 9. The KAPC Range Bin Power.

$$\text{Range Bin Power Centroid } RB_{PC} = \frac{\sum_{i=1}^{256} i x_i g_i(\theta_t = 0^o)}{RB_P}$$

$$\text{NOTE: } 1 \le RB_{PC} \le 256$$

Fig. 10. The KAPC Range Bin Centroid.

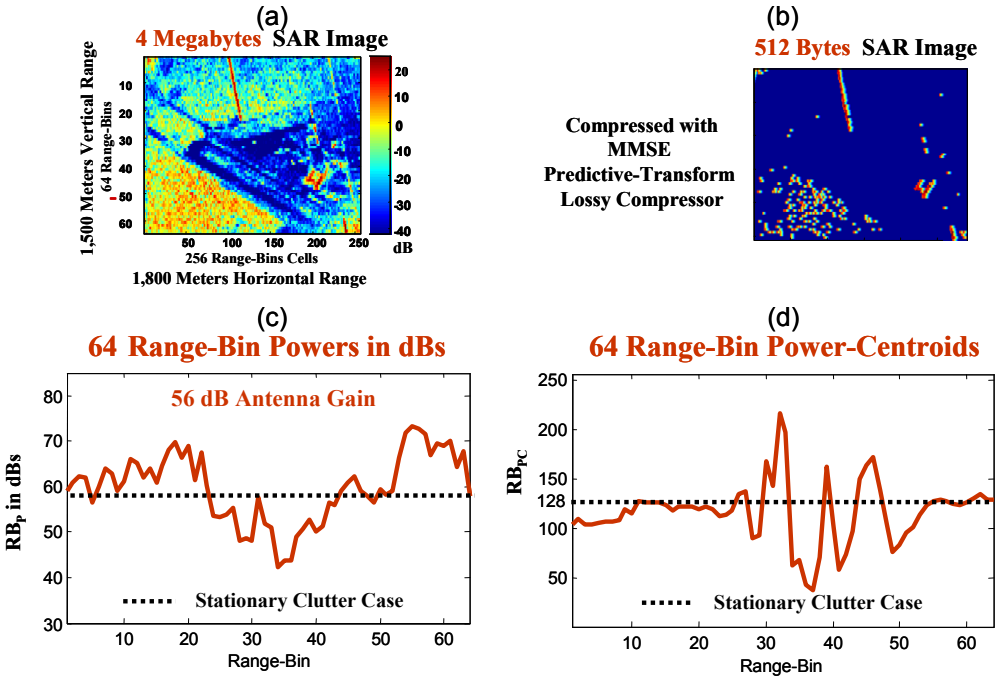

Fig. 11. The KAPC SAR Images and their Power and Power-Centroids.

For Example Below Three of these Covariances Found Off-line And Stored

$$^{CAP}C_c^f(Q(RB_{PC})) = \sum_{i=1}^{256} \mathbf{g}_i^{CAP}(\theta_t = \theta_C^{Q(RB_{PC})})\mathbf{c}_i(\theta_{AAM})\mathbf{c}_i^H(\theta_{AAM})$$

'Mathematical' Compensation Antenna Pattern (or CAP) Directed to Quantized Range Bin Centroid

Normalized CAP Illustration

Three CAPs (64, 128, 192) Example

$$Q(RB_{PC}) = \begin{cases} 64 & 1 \le RB_{PC} < 96 \\ 128 & 96 \le RB_{PC} \le 160 \\ 192 & 160 < RB_{PC} \le 256 \end{cases}$$

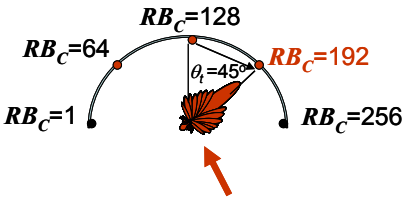

Normalized CAP $\{\mathbf{g}_i^{CAP}(\theta_t = \theta_C^{RB_C=192} = 45^o)\}$

Fig. 12. The KAPC Compensation Antenna Patterns (CAPs).

D. The 2009 Knowledge-Unaided Power Centroid (KUPC) Algorithm

The KUPC algorithm [1] is conveniently summarized in Figs. 13 and 14 where the KUPC NMxNM dimensional complex interference plus noise covariance matrix $^{KUPC}R_{xx}$ is the same as that for the KAPC algorithm with the exception that the range-bin power and power-centroid are determined on-line from $\sum_{i=1}^{K} \mathbf{X}_i\mathbf{X}_i^{\mathrm{H}}/K$, where this expression is a sample covariance matrix (SCM) that only uses samples from the range-bin under consideration. Moreover, due to the inherent robustness of range-bin power and power-centroid evaluations, reasonable estimates are expected to arise when a target is present on the range-bin under investigation. The KUPC algorithm is illustrated in Fig. 14 for the N=M=3 case which gives rise to the SCM 9x9 complex matrix shown in this figure. From this matrix RB_P is simply given by the real (1,1) element of the SCM with symbol m_1. On the hand, it is noted from the RB_{PC} algorithm displayed in Fig. 13 that to evaluate RB_{PC} the complex SCM elements (1,2) with symbol m_2, (1,3) with symbol m_3, (1,6) with symbol m_6 and (1,9) with symbol m_9 is all that is needed where: 1) N_c=NM=9 is the number of assumed range-bin cells; and 2) the constants k_2, k_3, k_4 and k_5 are for the example considered given by k_2=-60, k_3=30, k_4=-15 and k_5=7.5.

Power and Power-Centroid Derived from the SCM Correlation Elements

$$RB_P = m_1$$

m_1 is (1,1) Element of SCM

$$\frac{1}{K}\sum_{i=1}^{K}\mathbf{X}_i\mathbf{X}_i^H$$

$$RB_{PC} = \begin{cases} 1, & \overline{\mathbf{M}} < -\dfrac{N_C-1}{2} \\ \dfrac{N_C+1}{2} + \overline{\mathbf{M}}, & -\dfrac{N_C-1}{2} \le \overline{\mathbf{M}} \le \dfrac{N_C-1}{2} \\ N_C, & \dfrac{N_C-1}{2} < \overline{\mathbf{M}} \end{cases}$$

$$\overline{\mathbf{M}} = \sum_{i=2}^{N+M-1} k_i \mathrm{Imag}[m_i] \Big/ RB_P \qquad k_i = -60\,(-1)^i \frac{1}{2^{i-2}}$$

$$\{m_i : i = 2,..,N+M-1\} \text{ are elements of SCM}$$

Fig. 13. The KUPC RB_P and RB_{PC} Algorithms.

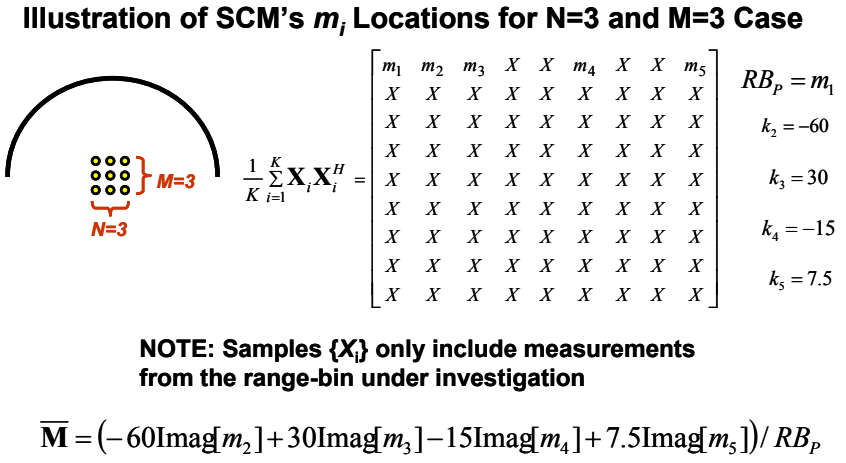

Fig. 14. The KUPC Sample Covariance Matrix.

E. Comparison of the SINR Performance of the Radar Schemes

In Fig. 15 a comparative study of the SINR performance derived with the SCMI, optimum SINR KASSPER, KAPC and fast KUPC (or FKUPC) adaptive radar algorithms is displayed where no jammers are assumed and the KAPC and FKUPC algorithms use 11 compensating antenna patterns or CAPs. In Table 1 the assumed radar parameters are given where the connection of these parameters to the covariance elements of the interference plus noise covariance model of Fig. 6 is documented in [1], [7]. In particular, it is noted from Fig. 15b that for range-bin #1 the SCMI scheme is in average 5.2 dBs away from the optimum SINR KASSPER performance, while for the KAPC and FKUPC schemes noticeably better results of approximately one dB are derived. These results are typical for all the 64 range-bins simulated as can be seen from Fig. 15c. Thus as noted in [1] the FKUPC algorithm advances the best possible practical results for adaptive radar since unlike the KAPC and KASSPER algorithms it is SAR imagery independent. Moreover, this powerful and fast scheme inherently surfaced from pursuing the novel LIT based *paradigm shift in signal processing design*, which, from first principles, seeks the replacement of a lossless signal processor whose input is compressed in a highly lossy manner with a *lossy* signal processor that is significantly better matched to the lossy input.

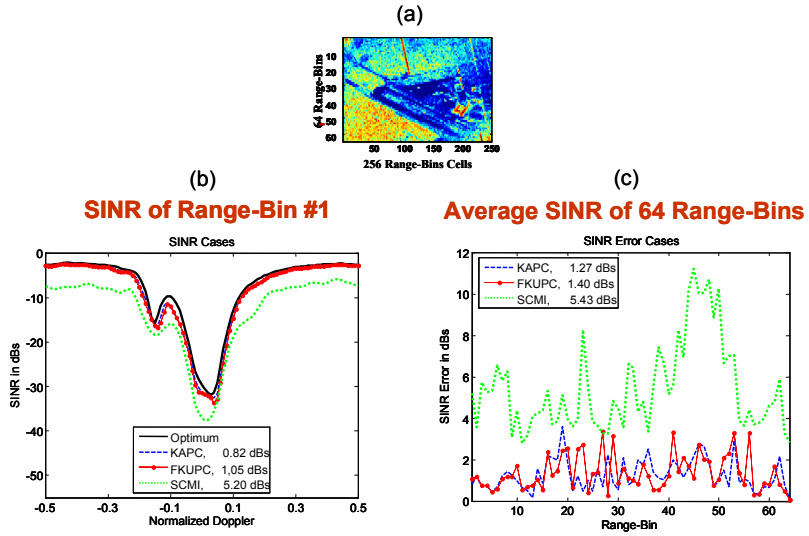

Fig. 15. No Jammers and 11 CAPs Case. (a) SAR image. (b) Range-Bin #1 Comparative Study. (c) All Range-Bins Comparative Study.

Table 1. Radar Simulation Parameters.

a.	Antenna	N=16, M=16, d/λ=½, $\sigma_n^2 = 1$ Front antenna gain constant: K^f = 56 dBs Back antenna gain constant: K^b = -40 dBs Carrier frequency: $f_c = 10^9$ Hz Pulse repetition frequency: $f_r = 10^3$ Hz Antenna array misalignment: $\theta_{AAM} = 2^o$
b.	Clutter	$N_c = 256$ Radar's *ratio*: $\beta = 1$
c.	Jammers	Jammers were used at -60°, -30° and 45° with 52, 55 and 66 JNRs in dBs, respectively, inclusive of antenna gains.
d.	Range Walk	Fraction of remaining area after range walk: ρ=0.999999.
e.	Internal Clutter Motion	Shape factor: $b = 5.7$ Wind-speed: $\omega = 15$ mph
f.	Channel Mismatch: Narrowband	Amplitude error: $\Delta\varepsilon_i = 0$ for all i, Phase-error: $\Delta\gamma_i$ fluctuates with a 5° rms for all i
h.	Channel Mismatch: Finite-Bandwidth	Amplitude peak deviation: $\Delta\varepsilon = 0.001$, Phase peak deviation: $\Delta\phi = 0.1^o$
i.	Channel Mismatch : Angle-Dependent	Bandwidth: B = 10^8 Hz Mainbeam width: $\Delta\theta = 28.6^o$

References

1. Feria, E.H., (2009) "On a nascent mathematical-physical latency information theory, Part I: The revelation of powerful and fast knowledge-unaided power-centroid radar", *Proc. of SPIE Defense, Sec. and Sen.. 2009,* Vol. 7351-29, pp. 1-18, *Orl., Fl.,* April 14, 2009. All the LIT publications can be retrieved from author's website.
2. _____ (2010) "Latency information theory: The mathematical-physical theory of communication-observation", *IEEE Sarnoff 2010 Symposium*, IEEE Catalog Number: CFP10PSS-CDR, ISBN:978-1-4244-5593-5, Library of Congress:2009910698, Princeton, New Jersey, 12-14 April 2010. LIT publications can be retrieved from author's website.
3. _____ (2010) "The latency information theory revolution, Part II: Its statistical physics bridges and the discovery of the time dual of thermodynamics", *Proc. of SPIE Defense, Security and Sensors 2010*, vol. 7708-30, pp. 1-22, Orlando, Florida, 4-6 April, 2010.
4. _____ (2009) "Latency information theory: A novel latency theory revealed as time-dual of information theory", *Proc. of IEEE Signal Processing Society:* DSP Workshop and SPE Workshop, Marco Island, FL, Jan. 2009.
5. Guerci, J.R. and Baranoski, E. (2006) " Knowledge-aided adaptive radar at DARPA", *IEEE Signal Processing Magazine*, vol. 23, no. 1, pp. 41-50, January 2006
6. Shannon, C. E. (1948) "A mathematical theory of communication", *Bell System Tech. Journal*, vol. 27, pp. 379-423, 623-656, July, Oct., 1948.
7. Feria, E.H. (2006) "A predictive-transform compression architecture and methodology for KASSPER," *FinalTechnical Report*, DARPA Grant FA8750-04-1-0047, May 2006.
8. _____ (2010) "The latency information theory revolution, Part I: Its Control Roots", *Proc. of SPIE Defense, Security and Sensors 2010*, Vol. 7708-29, pp. 1-8, Orlando, Florida, 4-6 April, 2010.
9. _____ (1985) "Matched processors for quantized control: A practical parallel processing approach," *International Journal of Controls*, Vol. 42, Issue 3, pp. 695-713, Sept. 1985.
10. Wozencraft, J.M. and Jacobs, I.M., (1965) "Principles of communication engineering," *Waveland Press,* Inc. 1965.
11. Bellman, R. (1957), *Dynamic programming*, Princeton University Press Dover paperback edition (2003).
12. Feria, E.H. (1994) "Decomposed predictive-transform estimation", *IEEE Trans. on Signal Proc.*, Vol. 42, No. 10, pp. 2811-2822, Oct. 1994.
13. Guerci, J.R. and Feria, E.H., (1996) "Application of a least squares predictive-transform modeling methodology to space-time adaptive array processing," *IEEE Trans. On Signal Processing,* pp.1825-1834, July 1996.
14. Mano, M.M and Ciletti, M.D., Digital Design, Prentice Hall, 2007.